RAA 2015 Vol. **15** No. **8**, 1414–1423 doi: 10.1088/1674–4527/15/8/021
http://www.raa-journal.org *http://www.iop.org/journals/raa*

Research in Astronomy and Astrophysics

A sample of E+A galaxy candidates in the Second Data Release of LAMOST Survey

Hai-Feng Yang[1,2,3], A-Li Luo[1], Xiao-Yan Chen[1], Wen Hou[1,3], Jian-Nan Zhang[1], Wei Du[1], Ji-Fu Zhang[2], Jiang-Hui Cai[2], Yan-Xin Guo[1,3], Shuo Zhang[3], Yong-Heng Zhao[1], Hong Wu[1], Ting-Gui Wang[4], Shi-Yin Shen[5], Ming Yang[1], Yong Zhang[6] and Yong-Hui Hou[6]

[1] Key Laboratory of Optical Astronomy, National Astronomical Observatories, Chinese Academy of Sciences, Beijing 100012, China; *hfyang@nao.cas.cn; lal@nao.cas.cn*
[2] School of Computer Science and Technology, Taiyuan University of Science and Technology, Taiyuan 030024, China
[3] University of Chinese Academy of Sciences, Beijing 100049, China
[4] Center for Astrophysics, University of Science & Technology of China, Hefei 230026, China
[5] Shanghai Astronomical Observatory, Chinese Academy of Sciences, Shanghai 200030, China
[6] Nanjing Institute of Astronomical Optics & Technology, National Astronomical Observatories, Chinese Academy of Sciences, Nanjing 210042, China

Received 2015 March 31; accepted 2015 May 26

Abstract A sample of 70 E+A galaxies is selected from 37 206 galaxies in the second data release of the Large Sky Area Multi-Object Fiber Spectroscopic Telescope (LAMOST). This sample is selected according to the criteria for E+A galaxies defined by Goto, and each of these objects is further visually identified. In this sample, most objects are low redshift E+A galaxies with $z < 0.25$, and are located in an area of the sky with high Galactic latitude and magnitude from 14 to 18 mag in the g, r and i bands. A stellar population analysis of the whole sample indicates that the E+A galaxies are characterized by both young and old stellar populations (SPs), and the metal-rich SPs have relatively higher contributions than the metal-poor ones. Additionally, a morphological classification of these objects is performed based on images taken from the Sloan Digital Sky Survey.

Key words: galaxies: evolution — galaxies: formation — galaxies: interactions — galaxies: peculiar — galaxies: starburst

1 INTRODUCTION

E+A galaxies, with strong Balmer absorption lines and little or no nebular emissions in their optical spectra, are widely considered to be a short-lived but potentially important phase in galaxy evolution (Leiva & Galaz 2014; Tran et al. 2003, 2004). The strong Balmer absorption lines (such as Hδ) indicate that the stellar population is dominated by A-type stars which must have formed within the last $\sim$1 Gyr. However, the lack of optical emission lines (such as Hα or [O II]) implies that star formation is not ongoing in these galaxies. A general interpretation of this spectral feature is that these galaxies are observed in a post-starburst phase (e.g. Dressler & Gunn 1983; Couch & Sharples 1987; Poggianti et al. 1999; Goto et al. 2003; Goto 2007b). But there are still some questions about this view, for example, they may also be produced by an abrupt truncation of star formation in their disk, without necessarily requiring a starburst (e.g. Shioya et al. 2004; Bekki et al. 2005). A lot of works have been dedicated to investigating the related physical mechanisms such as galaxy mergers (Mihos & Hernquist 1996; Bekki et al. 2005), interactions of physical pairs (Yamauchi et al. 2008; Matsubayashi et al. 2011; Bekki et al. 2005), interactions with a cluster tidal field (Poggianti & Wu 2000; Bekki et al. 2001) or intracluster medium (Bothun & Dressler 1986). However, the real scenario that can explain such galaxies is still uncertain.

In order to thoroughly understand the physics of E+A galaxies, a sample with a sufficient number of E+A galaxies is needed. However, one of the major difficulties is their rarity (Goto et al. 2003), and only sky surveys can provide the possibility of finding them. Recently, a catalog of E+A galaxies that included 564 objects was identified by Goto (2007a) from the Sloan Digital Sky Survey (SDSS) Data Release 5 (DR5). Seven very local E+A galaxies with $0.0005 < z < 0.01$ were discovered by Pracy et al. (2012) in SDSS DR7. In this paper, we present a sample of 70 local E+A galaxies carefully selected from the Large Sky Area Multi-Object Fiber Spectroscopic Telescope (LAMOST) Data Release 2 (DR2) (Cui et al. 2012; Zhao et al. 2012). This sample, together with available catalogs, can be used for statistical analyses and follow-up multiwavelength observations.

The paper is organized as follows. In Section 2, sample selection and an automated searching method are described in detail, and how to identify E+A galaxies is described. A preliminary discussion about this sample is shown in Section 3, including the space distribution, stellar population and image analysis. Finally, a summary is given in Section 4.

2 THE E+A GALAXY SAMPLE

2.1 LAMOST Dataset

The Large Sky Area Multi-Object Fiber Spectroscopic Telescope (LAMOST, also called the Guo Shou Jing Telescope) is a special reflecting Schmidt telescope with an effective aperture of 3.6–4.9 m and a field of view of 5°. It is equipped with 4000 fibers, with a spectral resolution of R $\approx$ 1800 and wavelength ranging from 3800 to 9000 Å (Cui et al. 2012; Zhao et al. 2012). The LAMOST DR2 (Liu et al. 2015), based on the pilot survey from 2011 October to 2012 June and the general survey from 2012 September to 2014 June, contains more than four million spectra with limiting magnitude down to V $\approx$ 19.5 mag (Luo et al. 2012). We take 37 206 spectra as the initial dataset which are spectroscopically classified as 'Galaxy' by the LAMOST 1D pipeline (Luo et al. 2015). In order to try to find as many E+A galaxies as possible, we keep spectra with low signal-to-noise ratio (SNR). Detailed steps used to search for E+A galaxies are described in the next subsection.

2.2 The Method Used for the Search

In the searching procedure, three characteristic lines (Hδ, Hα and [OII]) of E+A are considered to be selection criteria, the details of which are described in the following steps.

(1) 162 spectra with redshift $z > 1.18$ are removed since their Hδ lines are not within the spectral wavelength coverage of LAMOST.

(2) The spectra are shifted to the rest wavelength frame, and the Equivalent Widths (EWs) of Hδ, Hα and [O II] lines are roughly measured in the wavelength windows of 4082–4122 Å, 6553–6573 Å and 3717–3737 Å (Goto 2007a), respectively. If the [O II] double lines are not in the

optical wavelength range of LAMOST, the $EW_{[OII]}$ = 99; if the Hα line is not in this wavelength range, we set the $EW_{H\alpha}$ = 99 [1].

(3) Considering the uncertainty of EWs resulting from measurement errors, noise and estimation inaccuracy caused by using uniform-size wavelength windows for the various line widths of the spectra with lower SNR, our selection criteria for E+A galaxy candidates are temporarily relaxed by 0.5 Å compared to what were used by Goto (2004). Therefore, the galaxies with $EW_{H\delta} > 3.5$ Å, $EW_{H\alpha} > -3.5$ Å and $EW_{[O\,II]} > -3.5$ Å will be identified in the next step.

(4) The spectra satisfying the above conditions are individually visually inspected in this step. Those spectra with specific redshift in which Hδ or Hα are contaminated by sky lines or telluric lines are excluded. The spectra with redshift $z \in$ [0.383, 0.445] are also removed from our sample in this redshift range, because Hδ lines in these spectra are in the region where features might not be real because of low efficiency of the instrument in this range.

(5) The boundaries of the wavelength window defined by Hδ, Hα and [O II] are adjusted to maintain completeness of lines. Then, equivalent widths of these three lines are remeasured inside the adjusted wavelength windows.

(6) The final step in compiling the sample of E+A galaxies is to remove the objects with $EW_{H\delta} < 4$ Å, $EW_{H\alpha} < -3$ Å and $EW_{[O\,II]} < -2.5$ Å, which are the same criteria used by Goto (2007a). As a result, 70 E+A galaxies are finally identified.

2.3 Catalog of 70 Local E+A Galaxies

Table 1 lists the E+A galaxy sample selected from LAMOST DR2 by the method mentioned above, and Table 2 lists some corresponding photometric features. This first E+A galaxy sample from the LAMOST survey includes 70 objects, in which 56 of them are newly discovered. These E+A galaxies span a redshift range of $0.0034 \leq z \leq 0.2541$.

Table 1 The List of E+A Galaxies from LAMOST DR2

No.	Designation	Redshift	RA	DEC	$EW_{[O\,II]}$ (Å)	$EW_{H\delta}$ (Å)	$EW_{H\alpha}$ (Å)
1	J111058.63+284038.2	0.030500	167.744297	28.677292	23.485	4.838	1.125
2	J013936.61+294503.6	0.069828	24.902556	29.751000	–2.159	4.458	0.580
3^{+}	J105606.79+022818.5	0.151924	164.028320	2.471810	4.661	6.268	0.398
4	J040244.53+281212.0	0.049299	60.685553	28.203360	–1.222	4.738	0.792
5*	J131437.60+260726.2	0.073523	198.656698	26.123945	–2.768	4.134	0.573
6	J022954.96+031920.2	0.157351	37.479029	3.322285	–0.690	4.098	–0.840
7	J023255.55+023233.5	0.174831	38.231477	2.542655	–0.252	4.440	1.041
8^{*+}	J111742.26+042758.2	0.105046	169.426090	4.466180	–3.667	14.348	1.095
9	J023255.55+023233.5	0.174737	38.231477	2.542655	–0.649	4.218	0.945
10	J023351.45+023320.2	0.137500	38.464377	2.555622	–0.898	4.030	0.751
11	J023255.55+023233.5	0.174794	38.231477	2.542655	0.139	4.040	1.095
12^{*+}	J104349.87+420923.3	0.234008	160.957814	42.156500	1.051	5.747	0.827
13	J125006.26+452930.9	0.119162	192.526117	45.491935	1.876	4.303	0.809
14	J142744.06+345834.5	0.127800	216.933595	34.976265	2.554	4.625	0.442
15	J121837.19+403252.0	0.130000	184.654973	40.547788	2.334	4.059	1.660
16	J121711.03+411740.5	0.074964	184.295976	41.294593	3.128	4.851	1.149
17	J233000.39+031347.6	0.058616	352.501629	3.229915	–3.296	4.487	1.058
18^{+}	J233226.01+052135.7	0.069256	353.108400	5.359930	1.688	6.310	1.174
19	J024416.24+312200.0	0.017100	41.067678	31.366692	2.629	4.733	1.259
20	J013003.020025652.5	0.215250	22.512591	–2.947918	1.579	4.098	0.081
21	J012804.460041257.0	0.048006	22.018585	–4.215844	5.687	4.333	1.672

[1] Emission lines have a negative value throughout this paper and the value 99 indicates that this line should be neglected in selection.

Table 1 — *Continued.*

No.	Designation	Redshift	RA	Dec	$EW_{[O\,II]}$ (Å)	$EW_{H\delta}$ (Å)	$EW_{H\alpha}$ (Å)
22	J023103.93+014148.1	0.021150	37.766400	1.696709	3.212	4.125	1.377
23	J225648.87+052901.4	0.157710	344.203640	5.483740	2.007	4.031	0.469
24	J230536.08+053345.4	0.051679	346.400360	5.562620	1.364	4.107	1.221
25^{+}	J004025.91+052633.4	0.107554	10.107990	5.442630	–2.691	6.142	–0.325
26^{+}	J004053.76+052115.4	0.135811	10.224040	5.354280	3.218	5.072	0.522
27	J003409.66+084511.5	0.107989	8.540290	8.753200	–0.021	4.276	0.865
28	J001539.84+064100.6	0.069929	3.916040	6.683520	2.991	4.054	0.794
29	J012522.270003839.0	0.017848	21.342811	–0.644178	3.737	4.020	–0.604
30^{+}	J012730.400012319.5	0.016193	21.876671	–1.388775	–1.545	5.110	1.060
31^{+}	J021415.88+391627.4	0.082600	33.566198	39.274292	8.0724	7.095	–2.621
32^{+}	J021821.10+363113.9	0.037300	34.587923	36.520552	6.2058	5.308	0.791
33^{+}	J095530.30+255201.8	0.184076	148.876253	25.867171	–1.734	6.939	0.546
34	J023115.51+014119.7	0.022279	37.814643	1.688816	1.851	4.567	0.859
35^{*}	J091140.68+274111.2	0.157616	137.919525	27.686467	–1.870	4.383	1.770
36	J091000.34+274635.8	0.179827	137.501420	27.776630	–0.948	4.003	0.534
37	J012904.130034134.8	0.203008	22.267248	–3.693003	0.371	4.236	0.400
38^{+}	J012047.570033929.9	0.061524	20.198220	–3.658321	–0.445	6.026	0.984
39	J012633.050035540.4	0.198778	21.637733	–3.927915	–0.494	4.296	–1.417
40	J011908.930035346.3	0.131500	19.787224	–3.896207	0.203	4.780	0.875
41	J094106.78+344356.7	0.049757	145.278260	34.732440	1.197	4.367	1.038
42	J120329.26+023914.4	0.047823	180.871929	2.654006	–1.550	4.284	0.645
43^{*+}	J120419.070001855.9	0.093631	181.079480	–0.315540	–0.991	6.486	1.193
44	J091353.44+185630.4	0.032403	138.472670	18.941793	1.8432	4.160	1.327
45^{*+}	J104230.55+003441.9	0.100940	160.627319	0.578313	–1.482	5.968	–0.451
46^{*+}	J105755.26+334041.7	0.058130	164.480257	33.678251	–2.467	5.174	1.455
47	J104856.23+295406.7	0.197170	162.234310	29.901880	–0.087	3.945	0.726
48	J132556.100004208.6	0.055620	201.483756	–0.702390	0.407	3.952	0.997
49^{*}	J112844.18+234053.3	0.131520	172.184110	23.681485	–0.897	4.966	–0.026
50^{+}	J113108.88+230325.7	0.031260	172.787035	23.057152	2.351	5.095	0.780
51	J132318.78+130630.9	0.050370	200.828276	13.108591	0.631	3.570	1.005
52	J112512.50+262646.5	0.047500	171.302120	26.446264	0.917	4.202	1.451
53	J111728.76+275546.4	0.046750	169.369836	27.929575	–0.709	4.009	1.073
54	J132132.00+254816.8	0.225000	200.383358	25.804694	–0.756	4.246	1.101
55	J121351.590033521.5	0.080370	183.464961	–3.589329	–0.772	4.925	0.468
56	J151610.04+280412.3	0.111600	229.041840	28.070110	2.337	4.463	1.044
57^{+}	J114347.75+202148.0	0.022210	175.948994	20.363344	–0.899	5.121	1.634
58^{+}	J091903.75+322131.9	0.116387	139.765640	32.358870	–0.783	5.616	1.069
59	J120605.41+305637.1	0.023631	181.522582	30.943662	1.024	4.986	1.383
60^{+}	J151314.02+200951.2	0.038100	228.308423	20.164249	–2.271	5.845	–2.045
61	J152006.92+172848.2	0.096290	230.028860	17.480076	2.502	3.961	1.019
62^{*}	J141127.49+243809.5	0.053900	212.864561	24.635985	–0.756	4.648	1.016
63	J142850.16+310329.5	0.079250	217.209024	31.058200	0.541	4.024	0.810
64^{*}	J142848.23+274149.6	0.109590	217.200991	27.697123	0.221	4.530	1.341
65	J130008.02+274623.6	0.028640	195.033430	27.773226	–1.976	3.793	1.399
66	J125137.96+271838.4	0.024200	192.908190	27.310667	4.766	4.395	0.771
67^{*+}	J125717.81+274839.4	0.023580	194.324220	27.810959	3.407	5.095	1.586
68^{*+}	J124534.16+402559.3	0.081600	191.392350	40.433147	–0.922	5.882	1.294
69^{*+}	J151528.81+325813.4	0.100090	228.870056	32.970406	–0.535	5.852	1.147
70^{*}	J152426.50+080908.2	0.087130	231.110420	8.152294	–1.267	4.842	0.960

Notes: (1) 'No.' is the serial number for every object and it will be referred to throughout this paper. The items of Designation, Redshift, RA and DEC are obtained from catalogs associated with LAMOST DR2. (2) The '*' written as a superscript for serial number indicates that these objects have been published or are studied in other literatures. (3) The '+' written as a superscript for serial number indicates that the $EW_{H\delta} > 5.0$ Å.

Table 2 The Photometric Features of Our E+A Galaxy Sample

No.	Magnitude (mag)					$g-r$ (dex)	$r-i$ (dex)	Image Class
	u	g	r	i	z			
1	17.78	15.93	15.13	14.70	14.36	0.8	0.43	FOL1
2	18.84	17.04	16.32	15.97	15.71	0.72	0.35	FOL1
3	21.01	18.95	17.78	17.35	17.02	1.17	0.43	FOL2
4	-	-	-	-	-	-	-	-
5	17.62	15.79	15.04	14.71	14.46	0.75	0.33	FOL1
6	20.17	18.47	17.39	16.95	16.60	1.08	0.44	FOS2
7	19.73	17.93	17.03	16.65	16.41	0.9	0.38	FOS1
8	18.43	16.52	15.50	15.08	14.70	1.02	0.42	FOL2
9	19.73	17.93	17.03	16.65	16.41	0.9	0.38	FOS1
10	19.72	17.95	17.09	16.69	16.39	0.86	0.4	SGs
11	19.73	17.93	17.03	16.65	16.41	0.9	0.38	FOS1
12	19.44	18.04	17.18	16.93	16.75	0.86	0.25	SGs
13	19.04	17.21	16.44	16.12	15.83	0.77	0.32	FOL2
14	19.03	17.31	16.36	15.97	15.61	0.95	0.39	FOL2
15	20.10	18.31	17.39	17.02	16.71	0.92	0.37	FOL2
16	18.58	16.79	16.04	15.68	15.41	0.75	0.36	EOI
17	17.69	16.02	15.33	15.02	14.80	0.69	0.31	FOL1
18	19.59	17.64	16.76	16.34	16.02	0.88	0.42	FOS2
19	17.48	15.61	14.71	14.24	13.89	0.9	0.47	FOL1
20	20.65	18.64	17.64	17.30	17.07	1	0.34	FOS2
21	18.89	17.19	16.43	16.09	15.80	0.76	0.34	EOI
22	17.86	16.34	15.72	15.41	15.18	0.62	0.31	FOL2
23	20.30	18.40	17.34	16.88	16.55	1.06	0.46	FOL2
24	18.76	17.06	16.34	16.00	15.75	0.72	0.34	EOI
25	20.32	18.34	17.32	16.88	16.55	1.02	0.44	FOS2
26	19.30	17.48	16.64	16.28	15.99	0.84	0.36	FOS2
27	19.55	17.31	16.26	15.77	15.38	1.05	0.49	FOS2
28	18.83	17.20	16.53	16.21	15.95	0.67	0.32	SGs
29	18.90	17.39	16.67	16.32	16.09	0.72	0.35	FOS2
30	18.25	16.63	15.94	15.58	15.32	0.69	0.36	FOS2
31	-	-	-	-	-	-	-	-
32	-	-	-	-	-	-	-	-
33	19.49	17.96	17.27	16.98	16.84	0.69	0.29	FOS1
34	18.49	16.96	16.24	15.90	15.63	0.72	0.34	FOL2
35	18.91	17.13	16.54	16.22	15.98	0.59	0.32	FOL1
36	20.16	18.26	17.32	16.89	16.61	0.94	0.43	SGs
37	20.63	18.99	17.85	17.33	16.99	1.14	0.52	FOS2
38	21.19	19.12	18.18	17.77	17.44	0.94	0.41	FOS2
39	20.09	18.56	17.72	17.37	17.09	0.84	0.35	FOS2
40	18.97	17.42	16.74	16.42	16.17	0.68	0.32	FOS1
41	18.60	17.04	16.49	16.24	16.07	0.55	0.25	FOS2
42	19.16	17.54	16.86	16.55	16.30	0.68	0.31	EOI
43	17.59	16.08	15.61	15.45	15.24	0.47	0.16	SGs
44	17.07	15.41	14.79	14.48	14.26	0.62	0.31	FOL1
45	19.22	17.44	16.80	16.47	16.24	0.64	0.33	FOS2
46	19.49	17.71	17.09	16.78	16.57	0.62	0.31	FOS2
47	20.28	18.60	17.65	17.30	17.06	0.95	0.35	FOS2
48	18.40	16.77	16.13	15.84	15.61	0.64	0.29	FOS1
49	19.00	17.21	16.38	15.97	15.62	0.83	0.41	SGs
50	16.95	15.25	14.48	14.10	13.83	0.77	0.38	FOL2
51	19.05	17.41	16.70	16.36	16.13	0.71	0.34	FOS2
52	18.34	16.79	16.16	15.89	15.66	0.63	0.27	FOL1
53	19.11	17.35	16.58	16.21	15.93	0.77	0.37	FOS2
54	19.77	18.50	17.51	17.07	16.83	0.99	0.44	FOS2
55	18.40	16.97	16.46	16.20	16.00	0.51	0.26	FOS2
56	20.15	18.42	17.61	17.27	16.99	0.81	0.34	FOS2
57	17.54	16.13	15.66	15.42	15.26	0.47	0.24	SGs

Table 2 — *Continued.*

No.	Magnitude (mag)					$g-r$ (dex)	$r-i$ (dex)	Image Class
	u	g	r	i	z			
58	19.16	17.53	16.86	16.60	16.36	0.67	0.26	FOS1
59	19.63	18.06	17.43	17.12	16.90	0.63	0.31	FOL2
60	16.63	15.85	15.69	15.59	15.52	0.16	0.1	EOI
61	18.99	17.25	16.47	16.15	15.86	0.78	0.32	FOS2
62	17.91	16.63	16.21	16.00	15.82	0.42	0.21	FOL1
63	19.24	17.46	16.68	16.35	16.07	0.78	0.33	FOS2
64	19.09	17.45	16.82	16.59	16.39	0.63	0.23	FOL1
65	18.47	17.26	16.99	16.85	16.84	0.27	0.14	SGs
66	17.55	16.06	15.48	15.20	14.99	0.58	0.28	FOL2
67	17.55	16.03	15.50	15.25	15.06	0.53	0.25	FOL2
68	18.21	16.56	15.91	15.61	15.39	0.65	0.3	FOL1
69	19.66	17.98	17.35	17.05	16.83	0.63	0.3	FOS1
70	17.31	15.86	15.30	15.02	14.81	0.56	0.28	FOL1

Notes: (1) 'No.' is the serial number for every object and it will be referred to throughout this paper. The magnitudes in u, g, r, i and z bands, and colors $g-r$ and $r-i$ are obtained from the photometric catalog of SDSS. (2) We indicate '–' for three objects that do not have photometric information in the SDSS catalog. (3) The Image Class is visually assigned for each object based on material from Sect. 3.3.

In Table 1, each E+A galaxy is assigned a serial number (shown in column 1) that will be referred to throughout this paper and the superscripts indicate that these objects have been published or studied in other literatures. The other columns show the basic information on these objects including designation, redshift, RA, DEC, $EW_{H\delta}$, $EW_{H\alpha}$ and $EW_{[O II]}$. The redshift, RA and DEC are retrieved from catalogs associated with LAMOST DR2, and equivalent widths of these lines are measured by the method mentioned in the previous section.

Figure 1 shows six spectral examples of E+A galaxies, which correspond to the morphological classes in Figure 6, as described in Section 3.3. Table 2 lists the magnitudes in u, g, r, i and z bands, the colors $g-r$ and $r-i$, and image class by cross-matching these targets with the available SDSS photometric catalog (discussed in the next section).

3 DISCUSSION

3.1 Distributional Features of the Sample

Spatial distribution. The spatial distribution of E+A galaxies in our sample is shown in Figure 2. Most objects are located in areas with high Galactic latitude, but only a few of them are in the direction of the Galactic Anticenter. This may not accurately represent the true distribution of E+A galaxies because of the selection effect of the input catalog and the relatively small size of our sample.

Redshift distribution. The redshift distribution of E+A galaxies in our sample is shown in Figure 3. The average redshift is 0.0875 and about 65.5% of galaxies have redshift $z < 0.1$. The main reason is that LAMOST is probably more suitable for observations of nearby targets. We did not rule out the presence of a peak at $z \sim 0.04$ as described in Goto (2005), since the aperture of LAMOST may also bring introduce an aperture bias for nearby E+A galaxies due to their large sizes. Nevertheless, these local E+A galaxies, especially those with large apparent size, are suitable for more sophisticated researches such as morphology studies, substructure studies, and Integral Field Unit observations.

Magnitude distribution. Figure 4 shows the distributions of magnitude for E+A galaxies in our sample. The magnitudes of g, r and i bands for these objects are obtained by cross-matching with the SDSS photometric catalog. As seen in this figure, the magnitudes of g, r and i bands of most objects lie between 15 and 18 mag which is a good observational magnitude range for LAMOST.

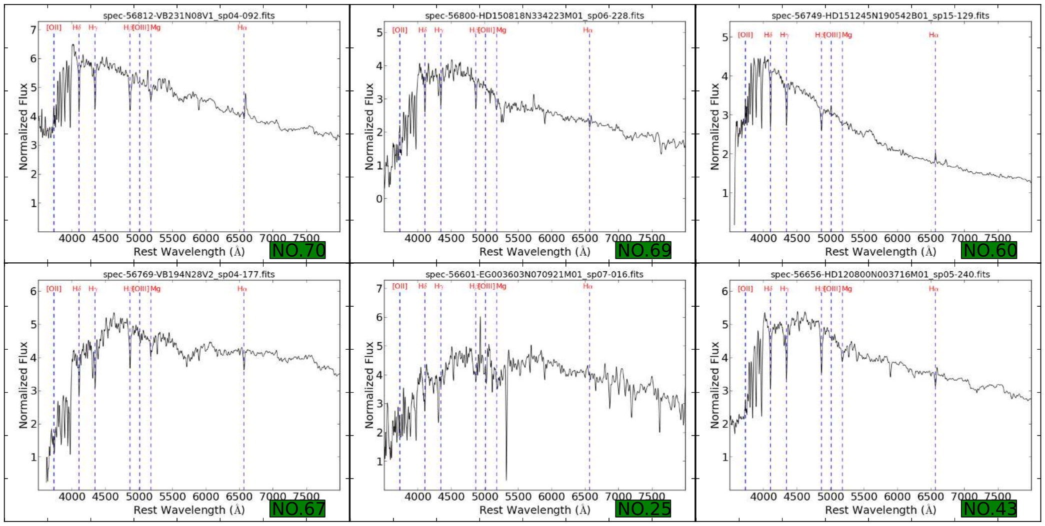

Fig. 1 Six example spectra from our E+A galaxy sample are shown in this figure. In order to clearly show the features, these spectra are smoothed to R∼1000 by a Gaussian function and shifted to the rest wavelength frame. Some typical lines are marked by green dashed lines and the serial number of each object is written in the bottom right corner.

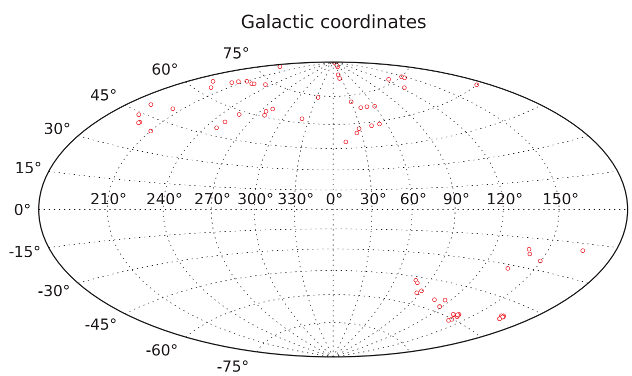

Fig. 2 This figure shows the spatial distribution of E+A galaxies selected from LAMOST DR2. These objects are marked by red circles in Galactic coordinates.

There are also some galaxies with both g and r bands fainter than 18 mag, however, they are too faint to resolve in the spectra because of their extremely low SNR.

3.2 Stellar Population Synthesis

Stellar population synthesis is performed for each spectrum by using the stellar population synthesis code ‘STARLIGHT’ (Chen et al. 2010). During the estimation, we restrict the wavelength range to 3700–8500 Å (in rest frame), and choose 45 Simple Stellar Populations, widely used in stellar population analysis, extracted from Bruzual & Charlot (2003) as templates. We use the Padova 1994

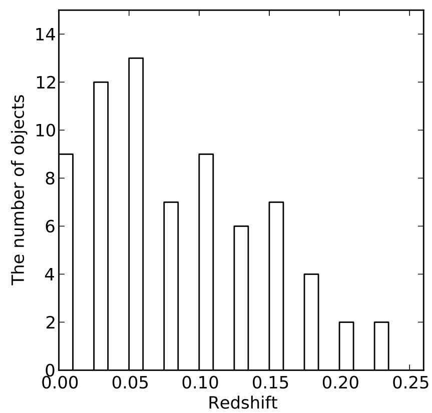

Fig. 3 A histogram of the redshift distribution of E+A galaxies in our sample. The bin size for redshift is 0.025.

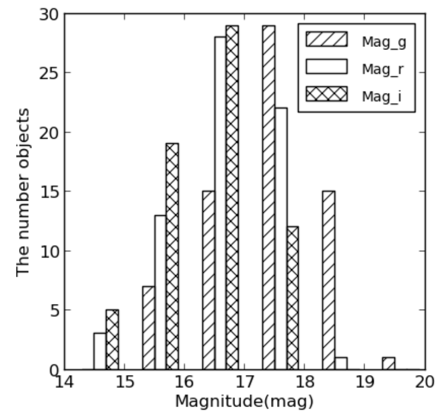

Fig. 4 Histogram of the distributions of magnitudes for E+A galaxies. The parallel slash, hollow and alternating slash bars represent the magnitude distributions of g, r and i bands, respectively.

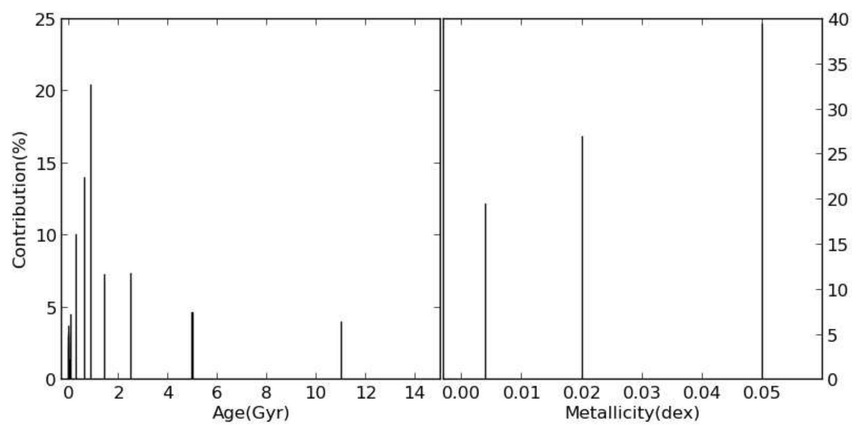

Fig. 5 The integrated age and metallicity contributions of all spectra in our sample estimated by 'STARLIGHT.' The left panel is the age (15 ages: 0.001, 0.003, 0.005, 0.01, 0.025, 0.04, 0.1, 0.3, 0.65, 0.9, 1.4, 2.5, 5, 11 and 13 Gyr) contributions and the right panel is the metallicity (3 metallicities: $Z = 0.004$, 0.02 and 0.05) ones.

tracks, the Chabrier (2003) initial mass function, and the Calzetti et al. (1994) reddening law. To understand the contributions of different stellar populations to the whole sample, age and metallicity contributions of all objects are integrated as shown in Figure 5.

The left panel of Figure 5 displays an obvious feature of young SPs with age of about 1 Gyr in the E+A galaxy spectra. In addition, old SPs with an age of about 11 Gyr also contribute to these E+A galaxies. This confirms that the selection criteria applied to E+A candidates are appropriate. The right panel of Figure 5 reveals that metal-rich SPs have relatively higher contributions than metal-poor ones.

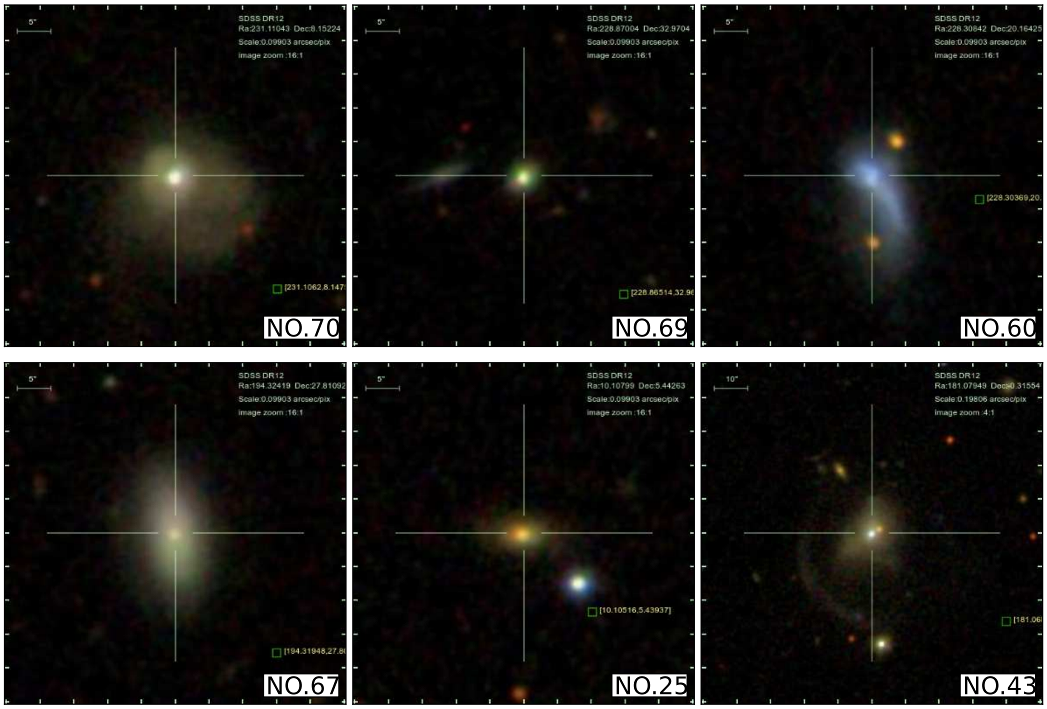

Fig. 6 Examples of composite images of E+A galaxies. The corresponding spectra are shown in Fig. 1. These images are sorted by image class as listed in Table 2. The first column shows FOL1 (*upper panel*, No.70) and FOL2 (*lower panel*, No.67); the second column shows FOS1 (*upper panel*, No.69) and FOS2 (*lower panel*, No.25); the third column shows EOI (*upper panel*, No.60) and SGs (*lower panel*, No.43).

3.3 Image Analysis

Many studies indicate that there are different features in the bulge, halo and disk of such special galaxies. We have obtained composite images of the E+A galaxies in our sample by cross-matching with the SDSS photometric catalog. We divided these images into four classes as seen in Table 2 and Figure 6.

(1) Face-On-Small (FOS) cases are E+A galaxies facing us with a projected size $<3''$.
(2) Face-On-Large (FOL) cases are ones facing us with a projected size $>3''$. For FOS and FOL E+A galaxies, FOS(FOL)1 indicates the galaxy has a very bright central bulge while FOS(FOL)2 means it does not.
(3) Edge-On/Irregular (EOI) cases are ones that we view edge on or are irregular galaxies.
(4) Special galaxies (SGs) are ones with some special features such as being lens-like.

4 SUMMARY

In this paper, we present a sample of E+A (post-starburst) galaxies based on the selection criteria $\mathrm{EW_{H\delta}} > 4.0$ Å, $\mathrm{EW_{H\alpha}} > -3.0$ Å and $\mathrm{EW_{[O\,II]}} > -2.5$ Å, which were described in Goto (2004). With such a threshold, 70 E+A galaxies are identified from LAMOST DR2. If we use a rigorous criterion of $\mathrm{EW}_{\mathrm{H}\delta} > 5.0$ Å, only 21 E+A galaxies remain which are specially denoted in Table 1. In addition, we exclude dozens of galaxies with $3.0\,\text{Å} < \mathrm{EW}_{\mathrm{H}\delta} < 4.0$ Å. These objects may also be an important evolutionary stage of E+A galaxies, especially for those with good signs of Hα and [O II] (i.e. they are absorption lines or extremely weak emission lines) in their spectra.

A preliminary analysis for this sample is carried out, including parameter distribution features, stellar population synthesis, and image classification. This sample, together with available catalogs, can be used for statistical analyses and follow-up observations in various wavelengths.

Acknowledgements This work is supported by the National Key Basic Research Program of China (Grant No. 2014CB845700), the National Natural Science Foundation of China (Grant Nos. 11390371, 11403036 and 11403059), and the Program for the Outstanding Innovative Teams of Higher Learning Institutions of Shanxi. The authors would like to thank the anonymous referee for many suggestions that have helped improve the manuscript. In addition, the authors are also particularly grateful for support from the AMD scholarship.

The Guo Shou Jing Telescope (the Large Sky Area Multi-Object Fiber Spectroscopic Telescope, LAMOST) is a National Major Scientific Project built by the Chinese Academy of Sciences. Funding for the project has been provided by the National Development and Reform Commission. LAMOST is operated and managed by National Astronomical Observatories, Chinese Academy of Sciences.

References

Bekki, K., Couch, W. J., Shioya, Y., & Vazdekis, A. 2005, MNRAS, 359, 949
Bekki, K., Shioya, Y., & Couch, W. J. 2001, ApJ, 547, L17
Bothun, G. D., & Dressler, A. 1986, ApJ, 301, 57
Bruzual, G., & Charlot, S. 2003, MNRAS, 344, 1000
Calzetti, D., Kinney, A. L., & Storchi-Bergmann, T. 1994, ApJ, 429, 582
Chabrier, G. 2003, PASP, 115, 763
Chen, X. Y., Liang, Y. C., Hammer, F., et al. 2010, A&A, 515, A101
Couch, W. J., & Sharples, R. M. 1987, MNRAS, 229, 423
Cui, X.-Q., Zhao, Y.-H., Chu, Y.-Q., et al. 2012, RAA (Research in Astronomy and Astrophysics), 12, 1197
Dressler, A., & Gunn, J. E. 1983, ApJ, 270, 7
Goto, T. 2004, A&A, 427, 125
Goto, T. 2005, MNRAS, 357, 937
Goto, T. 2007a, MNRAS, 381, 187
Goto, T. 2007b, MNRAS, 377, 1222
Goto, T., Nichol, R. C., Okamura, S., et al. 2003, PASJ, 55, 771
Leiva, R., & Galaz, G. 2014, in Revista Mexicana de Astronomia y Astrofisica Conference Series, 44, 179
Liu, X. W., Zhao, G., & Hou, J. L. 2015, RAA (Research in Astronomy and Astrophysics), 15, 1089
Luo, A.-L., Zhang, H.-T., Zhao, Y.-H., et al. 2012, RAA (Research in Astronomy and Astrophysics), 12, 1243
Luo, A.-L., Zhao, Y.-H., Zhao, G., et al. 2015, RAA (Research in Astronomy and Astrophysics), 15, 1095
Matsubayashi, K., Yagi, M., Goto, T., et al. 2011, ApJ, 729, 29
Mihos, J. C., & Hernquist, L. 1996, ApJ, 464, 641
Poggianti, B. M., Smail, I., Dressler, A., et al. 1999, ApJ, 518, 576
Poggianti, B. M., & Wu, H. 2000, ApJ, 529, 157
Pracy, M. B., Owers, M. S., Couch, W. J., et al. 2012, MNRAS, 420, 2232
Shioya, Y., Bekki, K., & Couch, W. J. 2004, ApJ, 601, 654
Tran, K.-V. H., Franx, M., Illingworth, G. D., et al. 2004, ApJ, 609, 683
Tran, K.-V. H., Franx, M., Illingworth, G., Kelson, D. D., & van Dokkum, P. 2003, ApJ, 599, 865
Yamauchi, C., Yagi, M., & Goto, T. 2008, MNRAS, 390, 383
Zhao, G., Zhao, Y.-H., Chu, Y.-Q., et al. 2012, RAA (Research in Astronomy and Astrophysics), 12, 723